

1 **Supplement of**

2 **Airborne bacteria viability and air quality: a protocol to quantitatively investigate the**  
3 **possible correlation by an atmospheric simulation chamber**

4  
5 *Virginia Vernocchi<sup>1</sup>, Elena Abd El<sup>1,2</sup>, Marco Brunoldi<sup>1,2</sup>, Silvia Giulia Danelli<sup>1</sup>, Elena Gatta<sup>2</sup>,*  
6 *Tommaso Isolabella<sup>1,2</sup>, Federico Mazzei<sup>1,2\*</sup>, Franco Parodi<sup>1</sup>, Paolo Prati<sup>1,2</sup>, Dario Massabò<sup>1,2</sup>*

7  
8 <sup>1</sup> INFN, Sezione di Genova, via Dodecaneso 33, 16146 Genova, Italy

9 <sup>2</sup> Dipartimento di Fisica, Università di Genova, via Dodecaneso 33, 16146 Genova, Italy

10

11 *Keywords:* bioaerosol, bacteria, Atmospheric Simulation Chambers, air quality

12 *\* Corresponding author:* Federico Mazzei; federico.mazzei@ge.infn.it

13

14

15 **S1: Details on the gas monitors installed at ChAMBRe**

16 The ENVEA-CO12e is a continuous carbon monoxide analyzer based on carbon monoxide detection  
17 by infrared light absorption measurement principle (EN 14626:2012, <https://store.uni.com/en/uni-en-14626-2012>). The concentration of CO in the sample is determined by measuring the quantity of  
18 infrared light, at the specific wavelength of 4.67 μm, absorbed by the sample gas as it flows through  
19 a multi-reflection chamber. The model available at ChAMBRe also features a built-in module for  
20 CO<sub>2</sub> monitoring (range: 0-2000 ppm by NDIR). The instrument has a sampling rate of approximately  
21 1 lpm, a response time of 20 s and a detection limit of 0.05 ppm.

22  
23 The measurement principle of ozone by the ENVEA-O342e is based on UV photometry (EN  
24 14625:2012 <https://store.uni.com/en/uni-en-14625-2012>). A 254 nm UV light signal is passed  
25 through the sample cell where it is absorbed in proportion to the amount of the ozone present  
26 (maximum range of ozone absorption 250-270 nm). Periodically, a zero-measurement is  
27 automatically performed by the device by switching between the sample stream and a calibrated  
28 ozone-free sample. The instrument has a sampling rate of approximately 1 lpm, a response time of  
29 20 s and a detection limit of 0.2 ppb.

30

31 The ENVEA-AF22e is based on ultraviolet fluorescence, which is the standard method for the  
32 measurement of SO<sub>2</sub> concentrations in ambient air (EN 14212:2012 <https://store.uni.com/en/uni-en-14212-2012>). A hydrocarbons scrubber guarantees the elimination of hydrocarbon interferences. The  
33

34 hydrocarbons free sample is sent to a reaction chamber to be irradiated by an UV radiation peaked at  
35 214 nm, which is the SO<sub>2</sub> molecule absorption wavelength. The fluorescence is optically filtered  
36 between 300 and 400 nm to eliminate some interfering gases. With a sampling rate of 0.4 lpm this  
37 instrument reaches a detection limit of 0.4 ppb with a response time of 20 s.

38

39 The ENVEA-C32e utilizes the principle of chemiluminescence, which is the standard method for the  
40 measurement of NO and NO<sub>2</sub> concentration (EN 14211:2012 [https://store.uni.com/en/uni-en-14211-](https://store.uni.com/en/uni-en-14211-2012)  
41 [2012](https://store.uni.com/en/uni-en-14211-2012)), for automatically analyzing the NO-NO<sub>x</sub> and NO<sub>2</sub> concentration within a gaseous sample.  
42 The analyzer measures the photons emitted after the reaction between NO and O<sub>3</sub>. The analyzer  
43 initially measures the NO concentration in the sample, through NO ozone oxidation. Subsequently,  
44 the sample passes through the heated molybdenum converter, which reduces NO<sub>2</sub> to NO and is then  
45 mixed with ozone in the reaction chamber and the resulting NO concentration is determined. In this  
46 way, the signal is proportional to the sum of the molecule NO and NO<sub>2</sub> (reduced to NO in the  
47 converter) in the sample. With a sampling rate of 0.66 lpm this instrument reaches a detection limit  
48 of 0.2 ppb with a response time of 40 s.

49

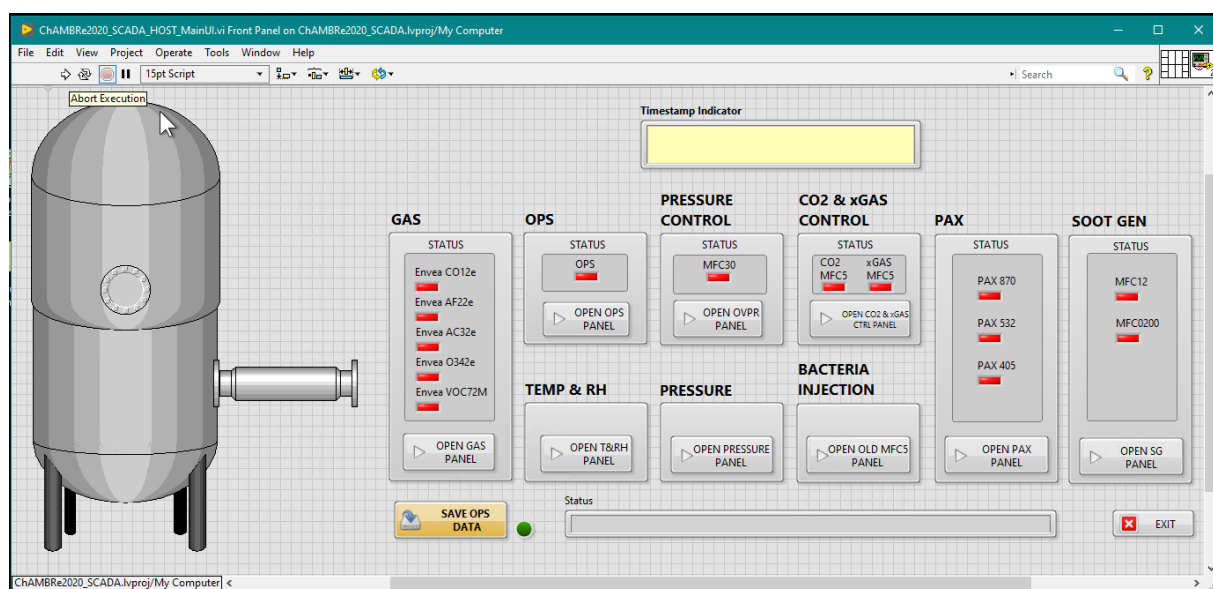
50 The ENVEA-VOC72e metrology, in accordance with EN 14662-3 ([https://store.uni.com/en/uni-en-](https://store.uni.com/en/uni-en-14662-3-2015)  
51 [14662-3-2015](https://store.uni.com/en/uni-en-14662-3-2015)). The VOC72e performs three main functions: the sampling, the GC analysis and the  
52 data processing. The sampling is achieved with a single trap filled with a specific sorbent. Its flow  
53 through the trap is about 12 mlpm which gives a sampled volume of 165 ml with the standard 15  
54 minutes cycle (sampling time >90% of cycle time). At the end of the sampling cycle, the trap is  
55 connected to the GC column and quickly heated from 35 to 380°C within 2 seconds. The compounds  
56 are thermally desorbed and flushed with hydrogen into the GC column. Then the trap is cooled with  
57 a fan for a new sampling cycle. Inside the GC column, the compounds are moved forward by the  
58 hydrogen flow (the mobile phase) and retained by the internal coating (the stationary phase) causing  
59 a selective retardation of the compounds. To achieve an optimal separation within a minimal time,  
60 the GC column follows a multi slope thermal cycle from a cold step (25°C) for the injection to a hot  
61 step (160°C) for flushing all the heavy compounds (i.e., compounds with a high boiling point). At the  
62 end of the hot step, the GC column is cooled to the cold step for the next cycle. The GC column  
63 output is connected to a photo ionization detector where the compound concentration is converted  
64 into a small electric signal. The PID detector includes a 10.6 eV UV lamp that ionizes all the  
65 compounds which ionization potential (IP) is less than 10.6 e V. The 240 V electric field between the  
66 polarization electrode (-240 V) and the signal electrode (at ground) moves the ionized particles  
67 (positive ions and negative electrons) towards the electrodes creating a small electrical conduction.

68 The resulting electric signal is amplified and digitalized in the electrometer board. Its recording gives  
69 the chromatogram which exhibits a peak for each detected compound. The standard measured  
70 compounds are Benzene, Toluene, Ethylbenzene, m+p-Xylene, o-Xylene, 1-3 Butadiene. Sample  
71 flow is around 50 mlpm, with a low detection limit of  $\leq 0.05 \mu\text{g m}^{-3}$  (benzene).

72

### 73 **S2: details on the custom SCADA acquisition and control system developed at ChAMBRé**

74 Figure S1 shows the main graphic user interface (GUI) of the NI LabVIEW custom application  
75 running continuously during the experiment. The status (on/off) of each sensor is shown on the main  
76 panel by a light indicator. Detailed information about each sensor is available by pressing the related  
77 subpanel button. The output data from all sensors are recorded at a user-selectable sampling rate  
78 (default: sampling rate =  $\text{s}^{-1}$ ). Time series can be visualized in real-time on the corresponding  
79 subpanel. During the experiment the user can also interactively set or modify several sensor  
80 parameters via the subpanel controls.



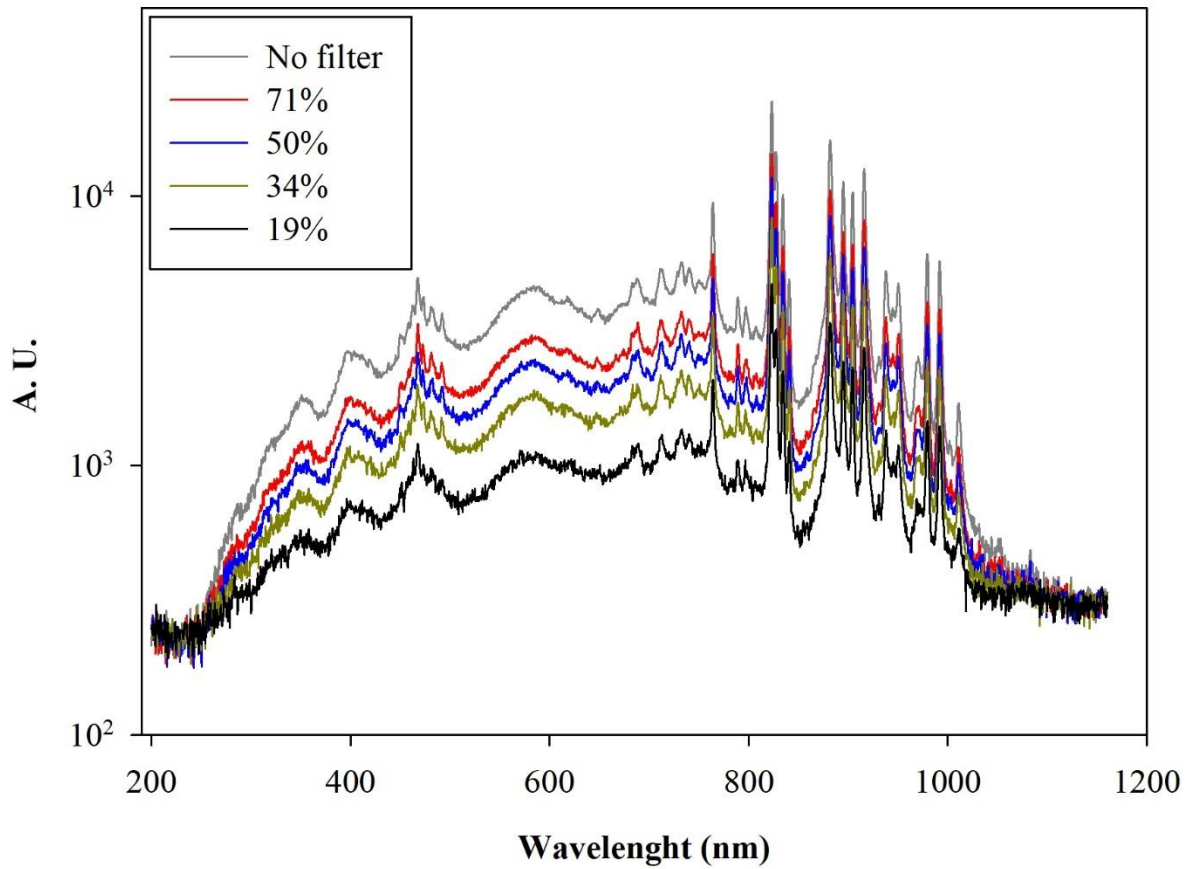
81

82 **Figure S1:** Screenshot of the graphic user interface of the SCADA application developed in LabVIEW™ language.

83

### 84 **S3: Feature of the Solar Simulator installed at ChAMBRé**

85 Several characterization measurements were carried out on the Solar Simulator. The device itself and  
86 its components were tested to assess the performance. Figure S2 shows a comparison of the effect of  
87 the four neutral density filters, which can provide attenuation up to 81% (filter labeled with 19% in  
88 the figure). The spectral features of the light produced by the Solar Simulator remain indeed  
89 unchanged after going through the neutral density filters, with the only appreciable difference being  
90 a uniform attenuation of the transmitted radiation.



92

93 **Figure S2:** Intensity vs wavelength measured with an Avantes ULS2048CL-EVO spectrometer directly at the exit of the  
 94 Solar Simulator with and without the available neutral density optical filters. The percentage reported in the legend is the  
 95 filter transmittance.

96

97 The stability of the Solar simulator has been measured over a period of 6 hours, resulting in a  
 98 maximum deviation (actually increase) of 6% in light intensity, likely due to the warming up of the  
 99 solar simulator lamp which takes nominally 20 minutes, but it is also subjected to small fluctuation  
 100 linked to the surrounding environmental conditions.

101

#### 102 **S4: details on the procedure to the optimum setting of the Quantum Tx counter**

103 The Quantum Tx has a factory standard counting protocol already preset, but several parameters must  
 104 be tuned on the characteristics of different bacterial species: Table S.1 reports the counting parameters  
 105 and the suggested factory settings for *E. coli*.

106

107

108

109

**Table S1:** Quantum Tx factory setting suggested for optimal counting for *E. coli*.

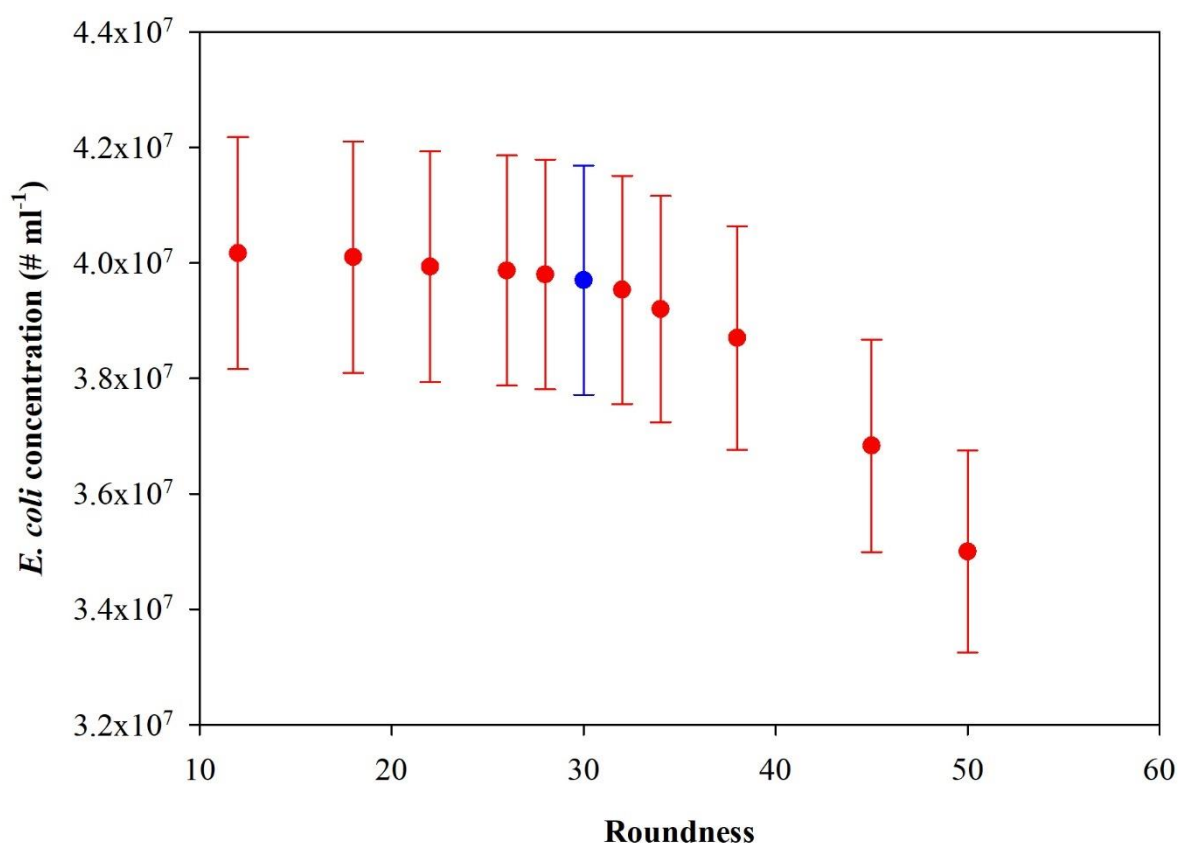
Parameter	Range	Default	<i>E. coli</i>
Dilution factor	1-20000	2	2
Min Fluorescent object size ( $\mu\text{m}$ )	0.3-49	0.3	1
Max Fluorescent object size ( $\mu\text{m}$ )	0.4-50	50	50
Roundness (%)	0-100	30	30
De-clustering level	0-10	7	7
Detection sensitivity	0-9	4	3

110

111 The *Dilution factor* must be set before counting and it is the ratio between the final volume of the  
 112 sample (bacterial suspension + reagents) and the volume of the bacterial suspension.

113 The *Fluorescent object size* measures the diameter of the fluorescent signal from the nucleic acid  
 114 stains. This does not correspond to the physical size of the cell. For the bacterial strain, used in our  
 115 experiments, the counts of fluorescent signals should be between 1 and 50  $\mu\text{m}$ . *Roundness* selects  
 116 cells based on their shape: the counting algorithm includes objects that are less round at lower values.  
 117 Higher values include rounder shapes. The *De-clustering* function allows for the efficient detection  
 118 of cells that may grow in clusters or chains. Higher values will lead to a higher sensitivity to clusters.  
 119 The last parameter, *Detection sensitivity* refers to the sensitivity of fluorescence detection. Higher  
 120 values detect fainter signals from weakly stained cells or smaller sample sizes but can also increase  
 121 noise. In our experiments, various measurements were made by raising and lowering the *Roundness*,  
 122 *De-clustering level* and *Detection sensitivity* parameters to verify if the standard protocol was optimal.  
 123 Below, the trend of *E. coli* bacterial concentration, varying the three parameters described above, is  
 124 shown. The *E. coli* concentration curve as a function of *Roundness* parameter shows a flat trend up  
 125 to a value of about 40% and then decreases rapidly for higher values: *E. coli* is a rod shape so high  
 126 *Roundness* values (i.e., sphericity of the object) lead to an underestimation of the total count.

127

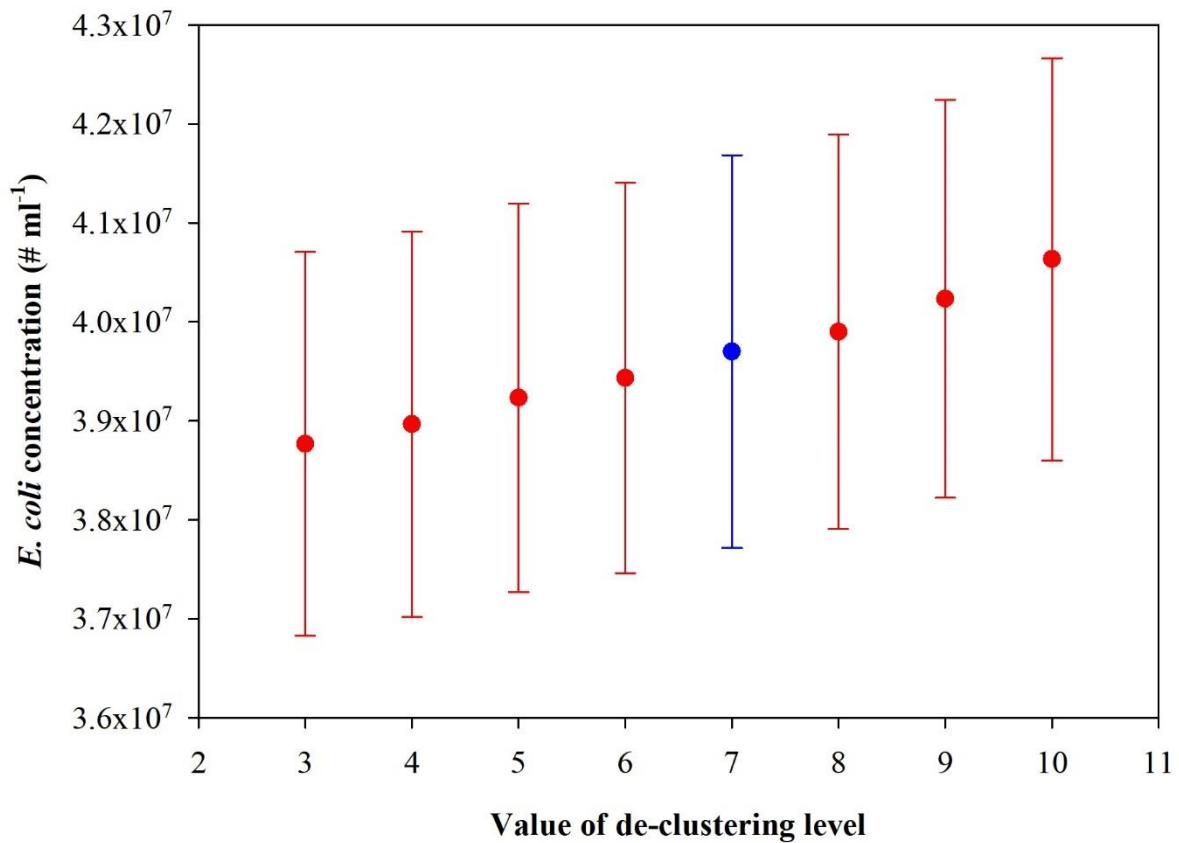


128

129 **Figure S3:** Trend of the *E. coli* concentration as a function of the change of the "Roundness" parameter. The point in blue  
 130 is the value obtained following the standard protocol for *E. coli*.

131

132 Figure S4 shows that the value of the bacterial concentration is not dependent on the variation of the  
 133 *De-clustering level*; this is probably because the images analyzed didn't show large agglomerations  
 134 or clusters. Anyway, raising this parameter, the count of bacterial concentration could increase due  
 135 to the ability of the instrument to separate clusters and individual components. However, it is worth  
 136 remembering that the clusters are usually probe agglomerates and, therefore, high value of *De-*  
 137 *clustering level*, could lead to include non-bacterial cells in the count.



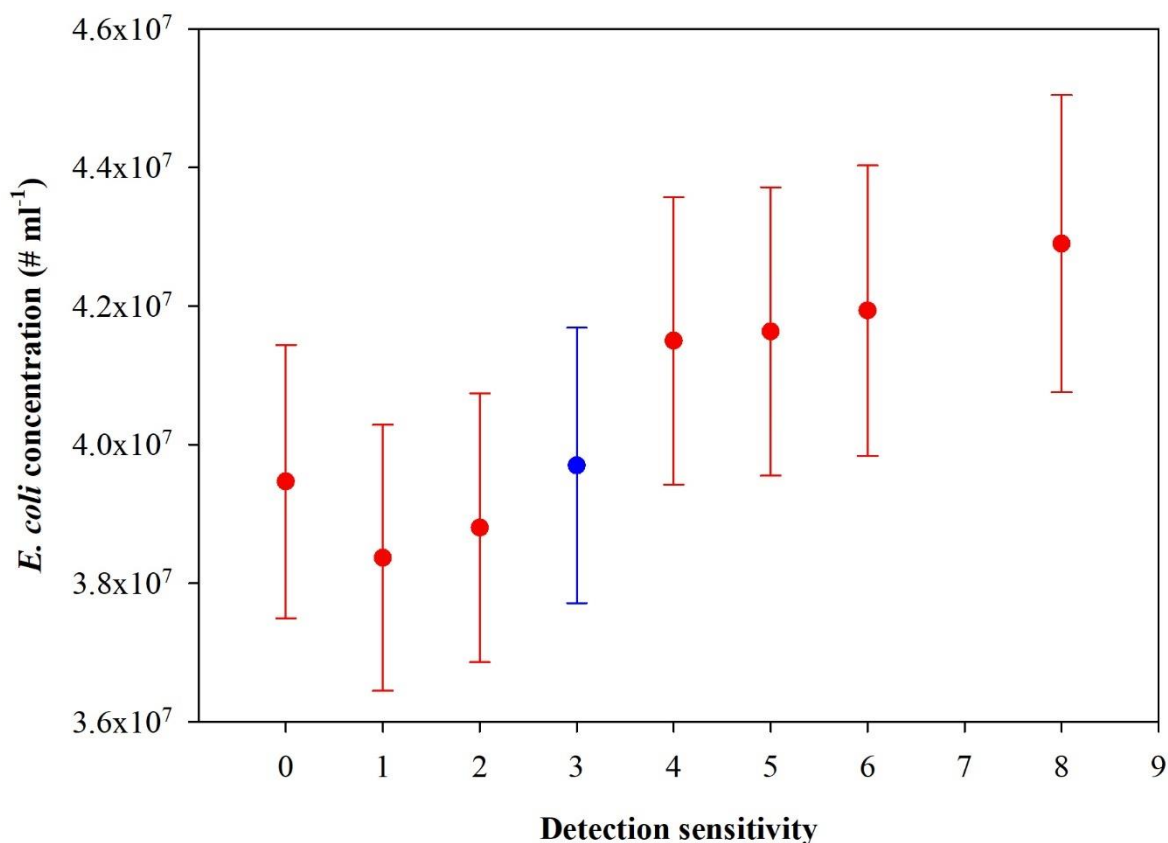
138

139 **Figure S4:** Trend of the *E. coli* concentration as a function of the change of the "De-clustering level" parameter. The  
 140 point in blue is the value obtained following the standard protocol for *E. coli*.

141

142 The *E. coli* concentration vs. *Detection sensitivity* shows the same trend as before; it is a flat curve as  
 143 the value of detection sensitivity changes. However, it is not recommended to select the lower or  
 144 higher value of detection sensitivity since some *E. coli* could be lost in the total count or the  
 145 background noise could increase, decreasing the quality of the images captured by the instrument,  
 146 respectively.

147



148

149 **Figure S5:** Trend of the *E. coli* concentration as a function of the change of the "Detection sensitivity" parameter. The  
 150 point in blue is the value obtained following the standard protocol for *E. coli*.

151

152 The results of these experiments showed that the variation of *Roundness*, *De-clustering level* and  
 153 *Detection sensitivity* does not affect the total bacteria concentration count (except for higher value of  
 154 *Roundness*) and the default protocol, suggested by the manufacturer, can be used without additional  
 155 adjustments.

156

157 **S5: reduction of *E. coli* viability measured in a set of experiments at ChAMBRé**

158

159 The experimental protocol discussed in the article is based on the monitoring, during the exposure to  
 160 the ChAMBRé atmosphere, of the concentration of viable bacteria by active sampling with a single-  
 161 stage Andersen impactor. The optimum sampling time to collect on the petri dishes in the impactor  
 162 a well countable number of bacteria (i.e., between 100 and 200 CFUs) while avoiding diluting too  
 163 much their concentration in the chamber was thoroughly investigated. During the experiment such  
 164 sampling time necessarily changes to consider the quite fast reduction of the bacteria (*E. coli*)  
 165 viability. Results are given in Table S2.

166 **Table S2:** Sampling time set for the Andersen impactor during the *E. coli* experiments for different time (in minute) after  
 167 the injection of bacteria.

Experiment	t: 0	t: 30	t: 60	t: 90	t: 120
Baseline dark	5 sec	10 sec	30 sec	1 min	1 min
NO <sub>2</sub> (900 ppb)	5 sec	30 sec	1 min	2 min	2 min
NO <sub>2</sub> (1200 ppb)	5 sec	30 sec	2 min	2 min	3 min
NO (900 ppb)	5 sec	30 sec	1 min	2 min	2 min
NO (1200 ppb)	5 sec	30 sec	1 min	2 min	2 min
Baseline light	5 sec	30 sec	1 min	2 min	2 min

168

169 Reduction in *E. coli* viability over time and with the ChAMBR<sub>e</sub> volume filled with a constant  
 170 concentration of a single pollutant are reported in Table S3. In all cases, the chamber was maintained  
 171 in darkness.

172

173 **Table S3:** Ratio of bacteria viable concentration during pollutants experiments and baseline experiments. Values indicate  
 174 the V:T ratio with pollutant and in the baseline experiment.

POLLUTANT (ppb)	Time after injection (min)				
	0	30	60	90	120
O <sub>3</sub> (>1000)	0.15 ± 0.06	0	0	0	0
NO <sub>2</sub> (900)	0.71 ± 0.19	0.37 ± 0.06	0.29 ± 0.05	0.14 ± 0.06	0.08 ± 0.03
NO <sub>2</sub> (1200)	0.37 ± 0.13	0.03 ± 0.01	0.01 ± 0.01	0.04 ± 0.03	0.01 ± 0.02
NO (900)	0.36 ± 0.12	0.13 ± 0.03	0.23 ± 0.04	0.47 ± 0.12	0.24 ± 0.07
NO (1200)	0.58 ± 0.19	0.25 ± 0.04	0.30 ± 0.05	0.45 ± 0.14	0.10 ± 0.04

175